FEBS Letters 580 (2006) 4551–4559

Expression and functional characterization of ABCG1 splice variant ABCG1(666)

Thomas Engel[a,*], Guenther Bode[a,b,1,2], Aloys Lueken[a,1,2], Markus Knop[c], Frank Kannenberg[a,b], Jerzy-Roch Nofer[a,b], Gerd Assmann[a,b], Udo Seedorf[a]

[a] *Leibniz Institute of Arteriosclerosis Research, Westphalian Wilhelms-University, Domagkstr. 3, 48149 Muenster, Germany*
[b] *Institute of Clinical Chemistry and Laboratory Medicine, Westphalian Wilhelms-University, 48149 Muenster, Germany*
[c] *Institute of Medical Biochemistry, Center for Molecular Biology of Inflammation, Westphalian Wilhelms-University, 48149 Muenster, Germany*

Received 26 May 2006; revised 3 July 2006; accepted 3 July 2006

Available online 13 July 2006

Edited by Sandro Sonnino

Abstract **The ATP-binding cassette transporter ABCG1 mediates the transport of excess cholesterol from macrophages and other cell types to high density lipoprotein (HDL) but not to lipid-depleted apolipoprotein AI. Several splice variants which may have different functions have been identified in mammals. In the current study, we characterized the human splice variant ABCG1(666), which differs from full-length ABCG1(678) by absence of an internal segment of 12 amino acids (VKQTKRLKGLRK). Accordingly spliced ABCG1 transcripts were detected in macrophages and liver in approximately twofold higher amounts than the alternatively spliced ABCG1 form encoding full-length ABCG1. We used transient and stable expression of ABCG1(666) fusion proteins to characterize glycosylation, subcellular localization, molecular interaction and functions of this ABCG1 variant. It could be demonstrated that ABCG1(666) is located at the cell surface and has the ability to form cholesterol transport competent homodimers which affect cellular cholesterol export in a similar manner as previously characterized forms of ABCG1. Our results support that ABCG1(666) may in fact be the most prominent form of functional ABCG1 expressed in the human.**

Keywords: ATP-binding cassette transporter; ABCG1; ABCA1; HDL; Cholesterol; Apolipoprotein AI

1. Introduction

High-density lipoprotein (HDL) acts in reverse cholesterol transport as acceptor of excess cholesterol secreted by peripheral cells for transport to the liver and subsequent excretion with the bile [1]. It is presumed that this role of HDL contributes importantly to the atheroprotective activity associated with this lipoprotein class [2,3]. ATP-binding cassette (ABC) transporters are energy-driven molecular pumps that are involved in transmembrane transport of a variety of substrates, including lipids, for a review see [4]. It has been shown that several members of this gene family are involved in sterol transport across the plasma membrane, including ABC transporter family member A1 (ABCA1), ABCG5, ABCG8, and ABC transporter family member G1 (ABCG1). ABCA1 catalyses the initial step of HDL-formation, the lipidation of lipid-free apolipoprotein AI (apoAI), and is essential for HDL-biogenesis. ABCA1 deficiency in Tangier disease results in almost complete lack of HDL, cholesterol ester accumulation in macrophages and a high incidence rate of premature atherosclerosis [5–7]. Mutations in the genes encoding ABCG5 and ABCG8 cause sitosterolemia [8], a rare recessive disorder associated with plant sterol and cholesterol hyperabsorption and premature atherosclerosis. To date, no human inherited disease has been identified that results from ABCG1 deficiency, however, ABCG1 has been studied in vitro in cell cultures and in vivo in mouse models. It could be demonstrated that overexpression of murine ABCG1 in cultured cells increased the rate of cellular cholesterol export to lipoprotein acceptors as well as to cyclodextrin but not to lipid-depleted apoAI [9,10]. Overexpression of two human ABCG1 transcripts differing at their N-terminal ends showed similar results [11]. In addition, that study attributed a role in cholesterol esterification to human ABCG1. Another study showed that human ABCG1 overexpression increased cholesterol efflux to a wide range of acceptors including phospholipid liposomes [12]. The strongest support for a role of ABCG1 in cholesterol transport in vivo came from the characterization of ABCG1 knockout mice. Although the phenotype was not associated with altered plasma HDL cholesterol or low-density lipoprotein (LDL) cholesterol levels, ABCG1 deficiency resulted in prominent cholesterol ester, triglyceride, and phospholipid storage in hepatocytes and macrophages within multiple tissues when mice were fed a high fat/high cholesterol diet. Transgenic mice overexpressing human ABCG1 showed opposite effects [13].

*Corresponding author. Fax: +49 251 83 57584.
E-mail address: engeltho@uni-muenster.de (T. Engel).

[1] These authors contributed equally.
[2] Present address: Institute of Experimental Dermatology, Westphalian Wilhelms-University, Röntgenstr. 21, 48149 Muenster, Germany.

Abbreviations: ABC, ATP-binding cassette; ABCA1, ABC transporter family member A1; ABCG1, ABC transporter family member G1; apoAI, apolipoprotein AI; BSA, bovine serum albumin; EGFP, enhanced green fluorescent protein; endoO, endoglycosidase O; endoH, endoglycosidase H; HA, hemagglutinin; HDL, high-density lipoprotein; HRP, horseradish peroxidase; LDL, low-density lipoprotein; LXR, liver-X-receptor; PNGaseF, *N*-glycosidase-F; RXR, retinoid-X-receptor

0014-5793/$32.00
doi:10.1016/j.febslet.2006.07.006

The first published ABCG1 cDNA contained an open reading frame of 638 amino acids [14]. Subsequently, a number of other ABCG1 isoforms that are generated by alternative splicing and/or promoter usage were identified. Full-length ABCG1 consists of 678 amino acids (ABCG1(678)) and is believed to represent the predominant form of ABCG1 expressed in human tissues. In this study we characterized a human ABCG1 splice variant, originally identified by Chen et al. [15], that differs from full-length ABCG1 by absence of an internal segment of 12 amino acids due to alternative splicing at the end of exon 17 [15,16] of the ABCG1 gene. We show that ABCG1(666) encoding transcripts are app. twofold higher expressed in human macrophages and the liver compared with ABCG1(678). In addition, we used transient and stable expression of ABCG1 fusion proteins to characterize glycosylation, subcellular localization, molecular interaction and functions of this ABCG1 variant.

2. Materials and methods

2.1. Reagents

Antibodies were purchased from Eurogentec (Herstal, Belgium; anti-hemagglutinin (HA), HA.11), Roche Diagnostics (Mannheim, Germany; mouse monoclonal anti-GFP), and Santa Cruz Biotechnology (Santa Cruz, CA, USA; rabbit polyclonal HA-probe, and rabbit polyclonal anti-GFP (SC-805 and SC-8334)). HRP-labelled secondary antibodies were from BioRad (Hercules, CA, USA). Liver-X-receptor (LXR) and retinoid-X-receptor (RXR) agonist T0901317 and RO-26-4456, respectively, were kindly provided by F. Hoffmann La-Roche (Basel, Switzerland), and used at a concentration of 0.1 and 1 μM, respectively. Glycosidases were obtained from Roche Diagnostics. An ABCG5-$(FLAG)_3$ plasmid was kindly provided by Dr. Helen Hobbs, UTSW Dallas, TX, USA [17].

2.2. Cells

HeLa cells (DSMZ, Braunschweig, Germany) were maintained in complete medium (DMEM/10% FCS/100 U/ml penicillin/0.1 mg/ml streptomycin) in a humidified incubator at 37 °C and 5% CO_2. Tet-Off-HeLa cells (BD Biosciences Clontech, Heidelberg, FRG) were maintained in complete medium supplemented with 0.2 mg/ml G418 sulphate in a humidified incubator at 37 °C and 5% CO_2. Stably transfected TetOff-HeLa cell lines were maintained in complete medium supplemented with 0.2 mg/ml G418 sulphate, 0.1 mg/ml hygromycin B, and 10 ng/ml doxycycline.

2.3. Preparation of lipoproteins

LDL ($1.019 < d < 1.063$ g/ml), HDL_2 ($1.063 < d < 1.125$ g/ml), and HDL_3 ($1.125 < d < 1.210$ g/ml) were isolated from plasma of normolipidemic volunteers by sequential ultracentrifugation [18] and were dialyzed against PBS. Lipid-free apoAI was purified from freshly isolated HDL_3 according to established procedures [19].

2.4. PCR amplification of ABCG1 splice product fragments

Human liver or monocyte-derived macrophage cDNA was amplified in a PCR reaction using HotstarTaq (Qiagen) and the following two primers: 5′-CTGAACTGCCCAACCTACCACAAC-3′; 5′-ATGATGCTGAGGAAGGTCCTCTTG-3′. 10% DMSO was added and 30 cycles were performed using the following thermocycler settings: 30 s at 94 °C, 40 s at 57 °C, 30 s at 72 °C. The PCR reaction was separated on a 2.5% agarose TAE gel and bands were visualized using ethidium bromide.

2.5. Cloning

Coding sequence of ABCG1(678) (NM_004915.2; bp 31–2055) ABCG1(666) (NM_016818.1; bp 31–2019), ABCG2 (NM_004827.1; bp 205–2172), ABCG4 (NM_022169.3; bp 337–2277), ABCG5 (NM_022436.2; bp 141–2096), and ABCG8 (NM_022437.2; bp 91–2112) were amplified from human cDNAs of different tissues with flanking *Xho*I at the 5′-end and *Xba*I (ABCG1, ABCG2, ABCG4), *Kpn*I (ABCG5), or *Bam*HI (ABCG8) restriction sites at the 3′-end and inserted in frame with enhanced green fluorescent protein (EGFP) into pEGFP-C1 vector (Clontech) or into a modified pEGFP-C1 vector where the GFP had been replaced by a triple repeat of the influenza virus hemagglutinin epitope tag (HA: YPYDVPDYA). Since cloning of correctly spliced ABCG5 failed repeatedly, ABCG5 was amplified using a plasmid coding for ABCG5-$(FLAG)_3$ as template [17]. Point mutations were introduced using QuikChange Kit according to the manufacturer's guidelines (Stratagene). All amplified sequences were verified by DNA sequencing using the ABI PRISM® BigDye™ Terminators v3.1 Cycle Sequencing Kit (Applied Biosystems). Sequencing reactions were separated on an ABI-PRISM 3700 DNA Analyzer (Applied Biosystems).

2.6. Expression of ABC transporters in HeLa cells

For transient expression experiments 1.6×10^6 trypsinized HeLa cells in 0.4 ml DMEM were transfected with 10 μg plasmid DNA using an electroporator equipped with a capacitance extender (GenePulser II, BioRad) at 975μF and 230 V. Cells were seeded on six 12 mm diameter cover slides in 24-well dishes and fixed with 4% PFA in PBS 48 h post transfection. Samples were counterstained with wheat germ agglutinin-Alexa® 594 (Molecular Probes, Leiden, The Netherlands). Coverslips were mounted on glass slides using Mowiol supplemented with *N*-propyl-gallate as anti-fading agent and were viewed with a Zeiss LSM510 confocal microscope. Images were processed using Adobe Photoshop 7.0. Stable transfections of TetOff-HeLa cells were performed as described above with 4×10^6 cells in 0.4 ml DMEM and 40 μg expression plasmid plus 2 μg pTK-Hyg (Clontech) selection plasmid. Cells were seeded in 10 tissue culture dishes with 15 cm diameter. For selection 0.2 mg/ml G418 (Gibco BRL), 0.2 mg/ml hygromycin B (Carl Roth, Karlsruhe, FRG), and 1 μg/ml doxycycline (Sigma) was added to complete medium. Medium was changed every 3–4 days, doxycycline was added every two days. Single clones were selected after 2–3 weeks using 8 mm cloning cylinders (Bellco Glass, Vineland, NJ), and screened by indirect immunofluorescence microscopy and Western blot analysis using the rabbit polyclonal anti-GFP or mouse monoclonal anti-HA.11 antibody, respectively. When plating the cells for experiments hygromycin B and G418 was omitted and doxycycline was used as indicated.

2.7. Immune precipitations

Cells were washed with PBS and washed off the plate in ice cold lysis buffer (50 mM Tris, pH 7.4, 150 mM NaCl, 1% (v/v) Triton-X 100) supplemented with protease inhibitor cocktail (Roche Diagnostics) plus 1 mM DTT and were lysed for 2 h on a rotating wheel at 4 °C. Supernatants were harvested by centrifugation and were precleared for 1 h using protein G-Sepharose 4B beads (Amersham Pharmacia Biotech, Freiburg, Germany). Antigen was immune precipitated by incubating the supernatants with mouse monoclonal anti-GFP IgGs prebound to protein G-Sepharose 4B beads for 2 h. Beads were harvested and washed five times with lysis buffer and processed for Western blot analysis.

2.8. Surface biotinylation

All steps were performed at 4 °C. One million cells in a 35 mm dish were washed twice with cold PBS and were incubated with PBS supplemented with 30 μg sulfo-NHS-biotin for 30 min. Cells were washed twice with PBS and unreacted biotin was quenched by 30 min incubation with Tris-buffered saline. Cells were washed off the plate in ice cold lysis buffer (50 mM Tris, pH 7.4, 300 mM NaCl, 0.5% (w/v) sodium deoxycholate, and 2% (v/v) Triton-X 100) supplemented with protease inhibitor cocktail (Roche Diagnostics) plus 1 mM DTT and were lysed for 2 h on a rotating wheel at 4 °C. Supernatants were harvested by centrifugation and were precleared for 1 h using protein G-Sepharose 4B beads (Amersham Pharmacia Biotech). Antigen was immune precipitated by incubating the supernatants with mouse monoclonal anti-HA IgGs prebound to protein G-Sepharose 4B beads for 2 h. Beads were harvested and washed five times with lysis buffer and processed for Western blot analysis using an goat anti-biotin antibody followed by donkey anti-goat HRP.

2.9. Glycosidase treatment

Immune precipitates from transiently transfected HeLa cells lysed with lysis buffer (50 mM Tris, pH 7.4, 300 mM NaCl, 0.5% (w/v) sodium deoxycholate, and 2% (v/v) Triton-X 100) were eluted from the protein G-beads with 0.1% (w/v) SDS, 1 mM 2-mercapto-ethanol, 50 mM Tris, pH 7.4 and aliquots were digested with different glycosidases in their respective digestion buffers according to the manufacturer's guideline (Roche Diagnostics). Before digestion Triton-X 100 was added to a 20-fold molar excess over SDS, 2-mercapto-ethanol was diluted to less than 0.1 mM. Reactions were incubated over night at 37 °C. Samples were precipitated with TCA, pellets were washed with acetone and dissolved in Laemmli sample buffer supplemented with 5% (v/v) 2-mercapto-ethanol (SDS-sample buffer) and processed for Western blot analysis. Anti-HA antibody was used for detection.

2.10. Western blot analysis

Samples were lysed in SDS-sample buffer and separated on 10% SDS–PAGE gels [20]. Protein was transferred onto Protran nitrocellulose filters, 0.2 μm pore size (Schleicher & Schuell, Dassel, Germany). For detection with HRP-labeled secondary antibody 2% (w/v) dry skim milk/PBS/0.1% (v/v) Tween 20 was used for blocking the filter and for antibody incubations, for detection of biotinylated proteins PBS/1 M NaCl/0.1% (v/v) Tween 20 was used for blocking and antibody incubations. For detection horseradish peroxidase (HRP)-labeled secondary antibody (BioRad), ECL system and Hyperfilm ECL was used (Amersham Pharmacia Biotech).

2.11. Cholesterol efflux measurement

Cholesterol efflux measurements were performed as previously described [21]. Cells were grown in a 24-well tissue culture plate. Confluent cells were labeled overnight with 0.5 ml/well of DMEM/0.2% (w/v) bovine serum albumin (BSA)/with or without agonists (1 μM T0901317 and 100 nM RO-26-4456) and 0.5 μCi [^{3}H]cholesterol (NEN-DuPont, Dreieich, Germany) per well. Cells were washed with warm DMEM/0.5% (w/v) BSA five times for 10 min each and with DMEM once. 0.3 ml efflux medium consisting of DMEM/0.2% (w/v) BSA with or without supplements (1 μM T0901317/100 nM RO-26-4456 with or without 20 μg/ml apoAI, 25 μg/ml HDL_3, HDL_2, or LDL) for several hours, as indicated. Medium was harvested, cells were removed by centrifugation and radioactivity of a 0.25 ml aliquot of the supernatant fraction was determined. Cells were lysed by adding 0.25 ml 1 M NaOH/0.15 M NaCl to each well of the plate. After 10 min lysates and pelleted cells were combined in scintillation vials, plates were washed again with 0.25 ml of 1 M NaOH/0.15 M NaCl and radioactivity of the samples was determined. The fractional cholesterol efflux was determined as described [21].

3. Results

The relative level of expression of alternatively spliced ABCG1 transcripts was determined by RT-PCR followed by agarose gel electrophoresis. As shown in Fig. 1A, RT-PCR with oligonucleotide primers flanking the 36 bp insertion/deletion resulted in two fragments of 277 (corresponding to ABCG1(666)) and 313 bp (corresponding to ABCG1(678)). Compared to ABCG1(678), ABCG1(666) encoding transcripts were more than twice as abundantly expressed in human monocyte-derived macrophages and liver. This observation was confirmed further by the result that during cloning of the ~2 kb coding sequence of the transporter from macrophage cDNA ABCG1(666) was obtained twice as often than ABCG1(678).

As NetNGlyc 1.0 server (http://www.cbs.dtu.dk/services/NetNGlyc/) predicted a glycosylation site in ABCG1(666) and ABCG1(678), we tested whether this site is functional in ABCG1(666). We expressed HA-tagged ABC transporters of the G-subfamily and digested anti-HA immune precipitates with different glycosidases. Fig. 1B shows that ABCG1(666) and ABCG4 are no glycoproteins. Neither endoglycosidase H (endoH), *N*-glycosidase F (PNGaseF), nor *O*-glycosidase (endoO) treatment shifted the molecular weight of ABCG1 or ABCG4. As positive controls, the weight of the highly glycosylated plasma membrane form of ABCG2 was lowered by PNGaseF- but not by endoH- or endoO-treatment and the weight of endoplasmic reticulum-retained ABCG5 was decreased by endoH- and PNGaseF- but not by endoO-treatment, as expected [17,22]. Since ABCG1(666) and ABCG4 are no glycoproteins, their intracellular transport

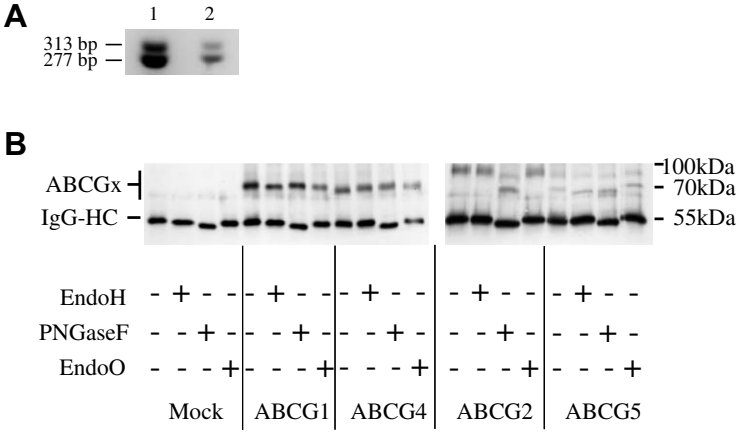

Fig. 1. Human ABCG1(666) internal short splice variant is more abundant than ABCG1(678) and is no glycoprotein. (A) Human monocyte-derived macrophage (lane 1) and liver (lane 2) cDNA was PCR-amplified with a primer pair adjacent to the internal alternative splicing site, as indicated in materials and methods. ABCG1 transcript lacking the internal dodecapeptide yielded a PCR product of 277 bp, whereas the alternative transcript was amplified as a 313 bp fragment. (B) HeLa cells were either mock-transfected or transfected with a plasmid coding for HA-tagged versions of the ABC transporters of the G subfamily for 48 h. Internally spliced short version, ABCG1(666), was used. Proteins were purified by immune precipitation and digested with different glycosidases, as indicated in panel B (EndoH, endoglycosidase H; PNGaseF, *N*-glycosidase F; EndoO, *O*-glycosidase). Samples were separated by SDS–PAGE and proteins were visualized by Western blot analysis, as stated in materials and methods using a rabbit polyclonal anti-HA antibody. The band at 55 kDa is IgG heavy chain (IgG-HC) and served as a loading control. Signals corresponding to the ABC-transporters are indicated with ABCGx at the left.

and localization could not be followed easily by analysis of post-translational modified intermediates.

In order to study intracellular trafficking and localization of ABCG1(666), we expressed ABCG1(666) and ABCG2 containing an HA epitope-tag or EGFP at their N-termini. As shown in Fig. 2A, the EGFP-ABCG1(666) and EGFP-ABCG2 fusion proteins were both detected at the plasma membrane. In addition, we could demonstrate that EGFP-ABCG1(666) and EGFP-ABCG2 both colocalized with Alexa®594-labeled wheat germ agglutinin, a marker for the plasma membrane (Fig. 2A). To rule out that ABCG1(666) was in close proximity rather than directly at the plasma membrane, we also performed surface biotinylation of living cells expressing $(HA)_3$-ABCG1 or $(HA)_3$-ABCG5 at 4 °C (Fig. 2B). $(HA)_3$-ABCG1 was biotinylated, whereas, as a control, $(HA)_3$-ABCG5, which is retained misfolded in internal endoplasmic reticulum membranes without coexpression of its partner ABCG8 [23], was not. Taken together, these results indicate that internally spliced ABCG1(666) is correctly targeted towards the plasma membrane.

Next, we analyzed the function of ABCG1(666) by testing cellular cholesterol efflux using TetOff HeLa cell lines stably expressing the transporter. We selected for doxycycline regulatable cell lines expressing ABCG1(666) homogenously as shown in Fig. 3. Fig. 4 shows the doxycycline dose response curve obtained for cholesterol efflux in the absence or presence of HDL_3 in the medium. Doxycycline concentrations of over ~100 pg/ml had no further decreasing effect on cholesterol export. Already at a doxycycline concentration of 10 pg/ml saturation of cholesterol export to BSA was observed, whereas HDL_3 export reached ~30% of the maximal effect. This difference most likely reflects the much lower cholesterol binding capacity of BSA than that of HDL_3. Cholesterol export depended on ABCG1 expression since ABCG2 expression was ineffective (Fig. 4). Overexpression of $(HA)_3$-ABCG1(666) in TetOff HeLa cell lines mediated export of cholesterol to a variety of extracellular acceptors in an acceptor independent manner (Fig. 5). Both, lipoprotein particles as well as serum albumin take up cholesterol twice as efficiently from wt ABCG1 expressing cells as compared to the same cell line where ABCG1 expression had been turned off by application of doxycycline, the parental TetOff HeLa cells or a cell line expressing inactive mutant ABCG1(666; K124M). ApoAI-mediated cholesterol efflux was essentially absent in the wt ABCG1(666) expressing cells. Phosphatidylcholine efflux was not significantly affected by overexpression of wt ABCG1(666) (not shown).

Since ABCG1(666) was detected at the cell surface and was functional, we assumed that the transporter was part of a full transporter, in analogy to results obtained for the heteromeric ABCG5 and ABCG8 complex and the homomeric ABCG2 [17,24,25]. Therefore, we performed non-reducing SDS–PAGE and subsequent Western blot analysis of samples containing wt or mutant $(HA)_3$-ABCG1(666) or $(HA)_3$-ABCG2. As shown in Fig. 6, in contrast to samples containing ABCG2, the ABCG1-containing ones showed presence of monomeric transporter, thus indicating that ABCG1 forms a full transporter without bridging through intermolecular disulfide bonds. Interestingly, in case of wt ABCG1 expressing samples a faint band at the expected dimeric weight of approximately 130 kDa was visible (indicated with an asterisk), even without chemical cross-linking, which was missing in the case of inactive ABCG1(666;K124M). This supported that the band of the dimeric size was not an artifact of over-

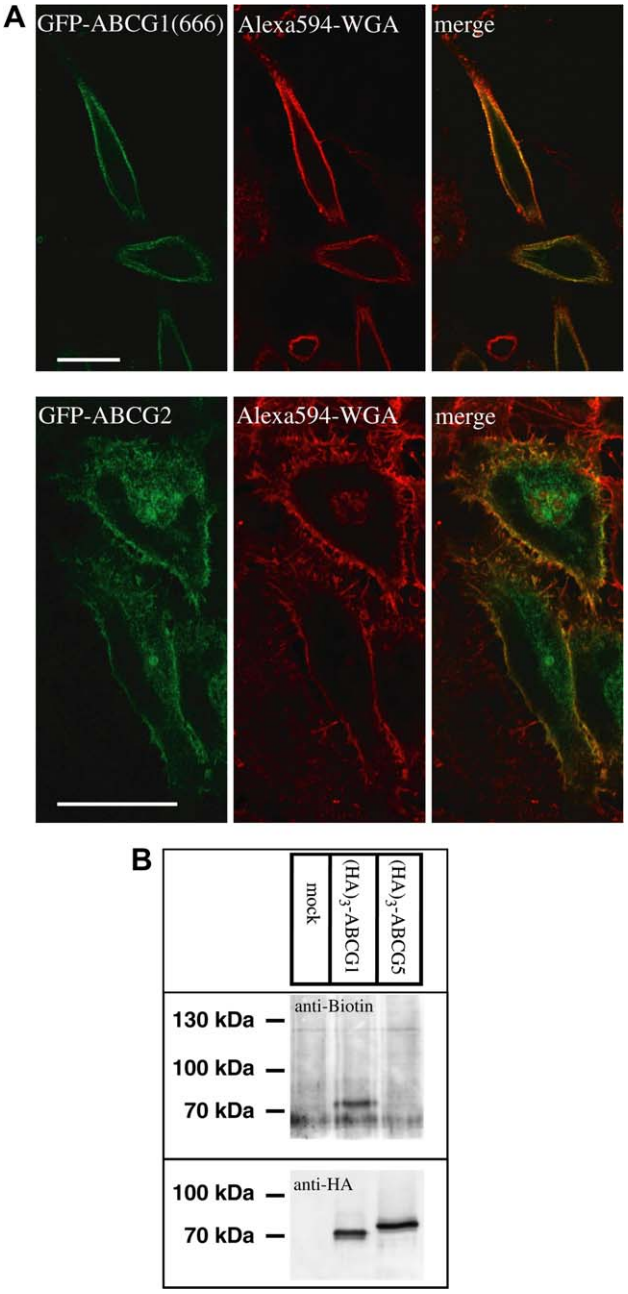

Fig. 2. ABCG1(666) colocalizes with wheat germ agglutinin (WGA) and can be biotinylated at the cell surface. (A) HeLa cells were transfected with constructs coding for EGFP-ABCG1(666) or EGFP-ABCG2 fusion proteins for 48 h. Cells were fixed with PFA and counterstained with WGA-Alexa® 594. Confocal sections show colocalization of EGFP-ABCG1 as well as ABCG2 with WGA at the cell surface. Green signals show EGFP epifluorescence, red signals show WGA-Alexa® 594, colocalization is indicated by yellow color in the merged image. Scale bars represent 25 μm. (B) HeLa cells were transfected with constructs coding for $(HA)_3$-ABCG1(666) or $(HA)_3$-ABCG5 fusion proteins for 48 h. At 4 °C living cells were surface biotinylated and after immune precipitation using the HA.11 antibody samples were separated by SDS–PAGE. An anti-biotin antibody followed by donkey anti-goat IgG-HRP detected biotin. ABC transporters in immune precipitates were detected using HA-probe followed by goat anti rabbit IgG-HRP. ABCG1 could be surface biotinylated, whereas ABCG5 could not.

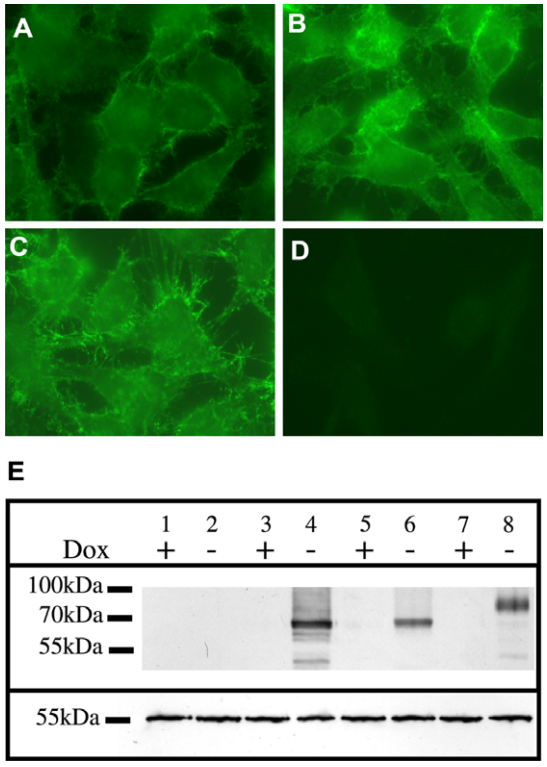

Fig. 3. ABCG1(666; K124M) mutant localizes at the cell surface and expression can be regulated by doxycycline. TetOff HeLa cells were stable transfected with plasmids coding for wt $(HA)_3$-ABCG1(666), mutant $(HA)_3$-ABCG1(666; K124M) or $(HA)_3$-ABCG2, respectively. Positive clones were selected and analyzed by indirect immunofluorescence microscopy using HA.11 antibody followed by an Alexa® 488-coupled goat anti-mouse IgG (A–D) or by Western blot analysis using HA.11 antibody followed by an HRP-coupled goat anti-mouse IgG (E). (A) Lanes 3 and 4: $(HA)_3$-ABCG1(666) clone 94. (B) Lanes 5 and 6: $(HA)_3$-ABCG1(666; K124M) clone 47. (C) Lanes 7 and 8: $(HA)_3$-ABCG2 clone 63. (D) Lanes 1 and 2: TetOff HeLa cells.

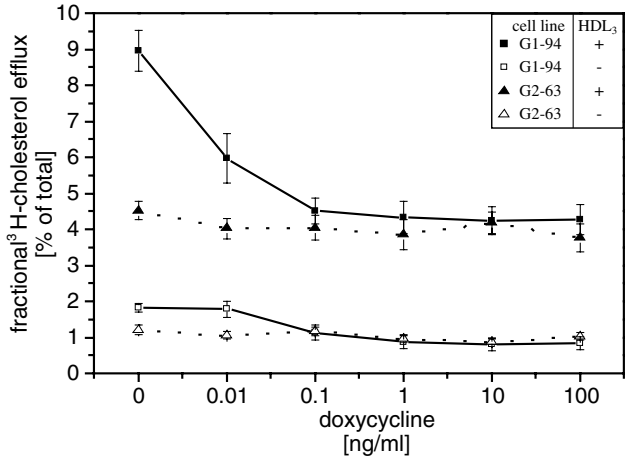

Fig. 4. Effect of doxycycline-dependent ABCG1(666) expression level on cholesterol efflux to HDL_3 and BSA. TetOff HeLa cell lines expressing $(HA)_3$-ABCG1(666) or $(HA)_3$-ABCG2 were labeled with [^{3}H]cholesterol and efflux to medium containing BSA or BSA plus HDL_3 was measured for 1.5 h, as indicated in Section 2. Doxycycline was used at the respective concentration shown. G1-94, $(HA)_3$-ABCG1(666) clone 94; G2-63, $(HA)_3$-ABCG2 clone 63.

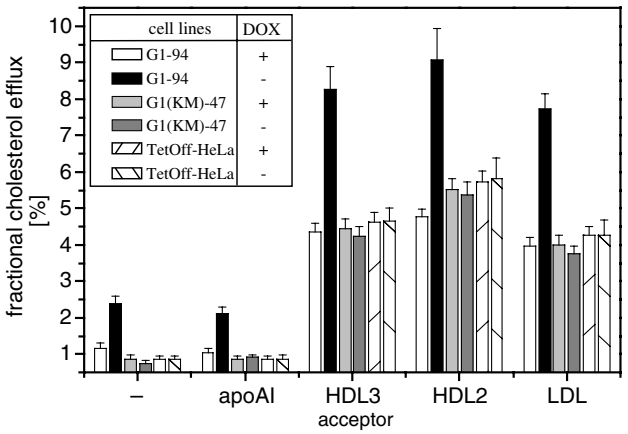

Fig. 5. Stable ABCG1(666) expression induces cholesterol efflux to various acceptors, except to lipid-free apoAI. [^{3}H]cholesterol efflux to various acceptors was measured for 1.5 h in TetOff HeLa cells either stably transfected with $(HA)_3$-ABCG1(666) (G1-94; white, black), $(HA)_3$-ABCG1(666; K124M) (G1(KM)-47; light/dark grey), or non-transfected (TetOff-HeLa; cross-hatched) in the presence (white, light gray, hatched) or absence (black, dark gray, hatched gray) of 1 μg/ml doxycycline, as described in Section 2.

expression but probably formed during conformational changes of the active transporter during its ATPase cycle that may expose internal cysteins. Application of LXR and RXR agonists did not influence the intensity of the dimeric band but seemed to have a protective effect on ABCG1 protein stability, because ABCG1 degradation products occurred less prominently when agonists were applied. Coexpression of the two ABCG1 splice variants ABCG1(666) and ABCG1(678) affected the signal intensity of the dimeric complex only marginally (Fig. 6B). The only difference was absence of the 55 kDa degradation product and appearance of a band at slightly higher molecular weight. This result may indicate that the two ABCG1 variants may in fact be able to form mixed complexes, which differ from homodimers by their accessibility to proteases.

Since these results indicated that the ABCG1 complex could not be easily analyzed by non-reducing gel electrophoresis we carried out analysis of immune precipitates of coexpressed ABC transporters of the G-family. We coexpressed all members of the G-family of ABC transporters with each other as HA- and GFP-tagged versions in various combinations and probed the anti-GFP immune precipitate with anti-GFP and anti-HA antibodies, as shown in Fig. 7. If interaction occurred, a signal should be present in the lower panel probed for hemagglutinin. In the case of EGFP-ABCG1 (panel A) predominantly interaction with HA-ABCG1 and to a small extent with HA-ABCG4 could be detected. In compliance with previous observations, ABCG2 formed homodimers (panel B), ABCG5 (panel D) and ABCG8 (panel E) formed heterodimers with each other [22,23]. ABCG4 formed homodimers and to a small extent heterodimers with ABCG1 (panel C).

4. Discussion

In the present study we characterized expression, molecular properties, localization and function of a previously identified human ABCG1 transcript which, due to alternative splicing,

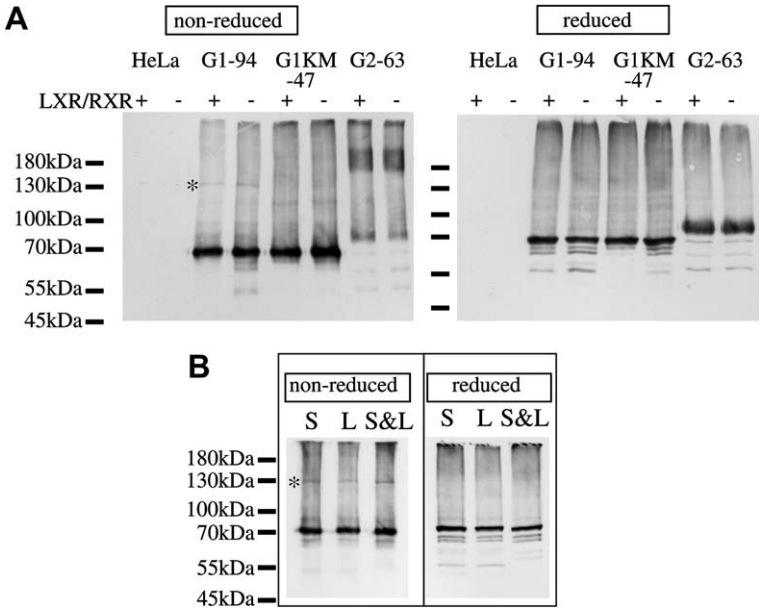

Fig. 6. Disulfide bonds do not link ABCG1(666) full transporter. (A) Samples from TetOff HeLa cell lines expressing wt or mutant (K124M) $(HA)_3$-ABCG transporter, as indicated, were subjected to reducing (right panel) or non-reducing (left panel) SDS–PAGE and subsequent Western blot analysis with HA.11 antibody followed by goat anti-mouse HRP-labeled secondary antibody. An asterisk indicates a putative dimeric ABCG1 complex. G1-94, $(HA)_3$-ABCG1(666) clone 94; G1KM-47, $(HA)_3$-ABCG1(666, K124M) clone 47; G2-63, $(HA)_3$-ABCG2 clone 63. (B) Samples from TetOff-HeLa cells containing transiently expressed $(HA)_3$-ABCG1(666), indicated with S, or $(HA)_3$-ABCG1(678), indicated with L, or a combination of both were processed as above.

differed from previously characterized ABCG1 variants by absence of an internal segment of 12 amino acids (Fig. 8). The studied human cell-types liver and monocyte-derived macrophages, that were previously shown to contain large amounts of ABCG1 [13], provided considerably more intense signals corresponding to transcripts encoding the ABCG1(666) form with the 12 aa deletion than to full length ABCG1(678) (Fig. 1A). The expressed sequence tag database at the NCBI confirms this observation with a ratio of five long (DA278-234.1, AA860987.1, DA255931.1, BQ640204.1, AW467144.1) versus 10 short internally spliced transcripts (DA382048.1, DA464214.1, BX419732.2, CD628158.1, CD628157.1, CD62-8156.1, BF871693.1, BX427799.2, CD628159.1, BG74717-1.1). The long transcript may occur in humans only, as the non-redundant database (NR) at the NCBI contains ABCG1 sequences in other species spliced comparable to the short ABCG1(666) variant only (Fig. 8A). In addition, the human ABCG4 transcript, the closest homolog of ABCG1 [26], has a similar sequence gap at the same position (Fig. 8A). This suggests that ABCG1(666) may in fact be the most prominent form of ABCG1 expressed in humans.

Alternative splicing represents an attractive mechanism for expression of functionally diverse products from a single gene. A potentially regulatory role mediated by gene silencing has for example been attributed to a non-functional form of P-glycoprotein resulting from alternative splicing upon ABCB1 transcription [27]. In *Drosophila melanogaster*, alternative internal splicing at positions between exon 4 and exon 8 of dMRP has been reported to result in as many as 14 different proteins [28]. Although the precise role of this variation, which occurs within the second and third membrane-spanning domain of the transporter, is currently unclear, it seems likely that it contributes to the broad substrate specificity required for dMRP function. Alternative internal splicing of the human ABCB4 (MDR3) cDNA was reported as well, however without effect on the protein sequence [29]. In the case of SUR2 (ABCC9), two functional variants have been described, which differ with respect to the first nucleotide binding fold of the transporter based on absence or presence of exon 17 coding information in the spliced transcripts [30].

Since our results show very clearly that ABCG1(666) encodes a functional ABC transporter, a regulatory role as has been proposed in case of the alternatively spliced form of P-glycoprotein may be excluded for ABCG1(666). Our data rather support that the 12 aa deletion does not interfere with the basic cholesterol export function of the transporter. According to the multiple sequence alignments of homologous and orthologous peptide sequences similar to human ABCG1 at the position flanking the insertion/deletion shown in Fig. 8A, the insertion may occur specifically in humans, since the non-redundant database (NR) at the NCBI contains only ABCG1 sequences of mouse, rat, dog, cattle and zebrafish which are spliced according to the short ABCG1(666) variant. In addition, the human ABCG4 transcript, the closest homolog of ABCG1 [26], has a similar sequence gap at the same position (Fig. 8A). Further analysis with the DISEMBL program (http://dis.embl.de/) supports that this stretch of sequence and the adjacent region has a highly unordered structure (indicated as hotloop and disordered) and, therefore, may act as a flexible linker connecting the ATPase and transmembrane spanning domain of the transporter (Figs. 8A and B). Based on these considerations, we presume that ABCG1(666) represents the evolutionary conserved prototype transporter whereas ABCG1(678) may be a primate-specific variant that arose later in evolution.

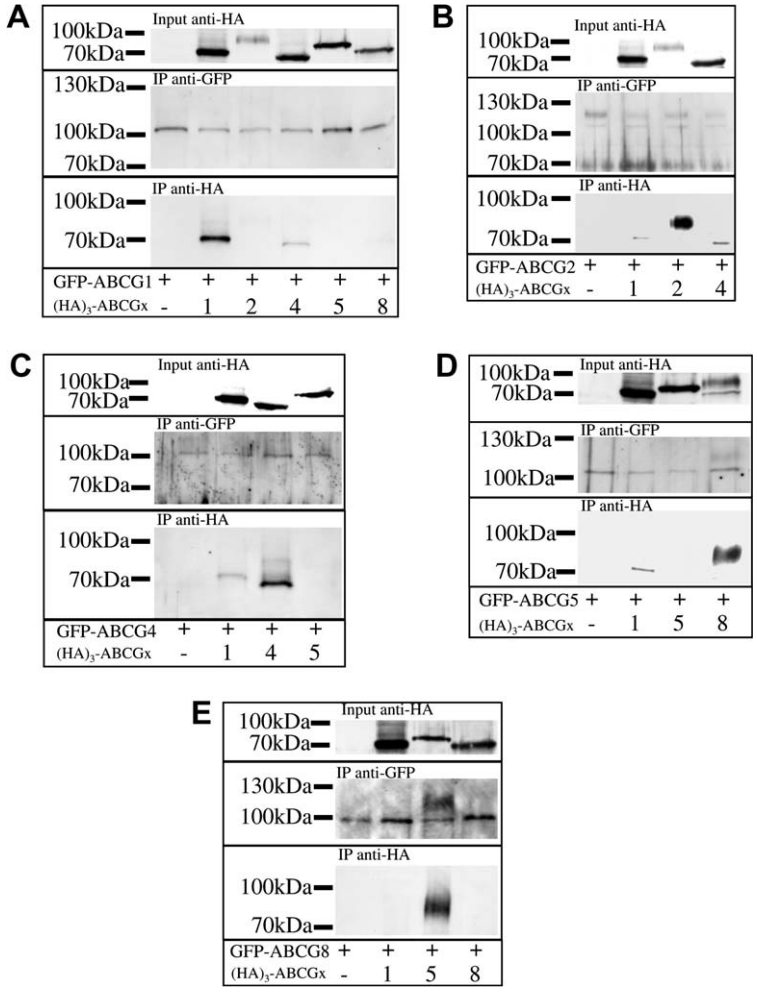

Fig. 7. ABCG1 interacts with itself. HeLa cells were cotransfected with a combination of one HA-tagged and one GFP-tagged ABC transporter of the G-subfamily or only one of them. After lysis, GFP-tagged ABC transporters were immune precipitated and HA- as well as GFP-tagged proteins were detected by Western blot analysis. Interaction of ABC transporters with each other is evident, if protein in the anti-GFP precipitate can be detected using the anti-HA antibody. The following fusion proteins were used as baits: panel A: EGFP-ABCG1(666); panel B: EGFP-ABCG2; panel C: EGFP-ABCG4; panel D: EGFP-ABCG5; panel E: EGFP-ABCG8.

Despite the fact that our results seem to indicate that the basic properties and activities of ABCG1(666) are in fact very similar as compared with previously characterized ABCG1 variants containing the 12 aa insertion, our data also point to a number of potential differences that may exist between the ABCG1 isoforms. In our study, ABCG1(666) expression was not associated with stimulation of cholesterol esterification as was observed by Vaughan and Oram who expressed two ABCG1 variants containing the 12 aa insertion in BHK cells [11]. Gelissen et al. expressed ABCG1(674), a variant also containing the 12 aa insertion, in CHO cells [12]. They found the majority of the expressed protein intracellularly associated with the endoplasmic reticulum and not, as in our case, within the plasma membrane. These differences may relate to subtle distinctions with respect to the precise intracellular trafficking routes and/or the efficacy by which the transporters are directed towards the plasma membrane. On the other hand, there clearly are a number of experimental differences between the studies. Vaughan and Oram used an N-terminal tag in their experiments similar as we did, whereas Gelissen et al. tagged the expressed transporter at its C-terminus [11,12]. It is known for other ABC transporters of the G-family that the location of the tag influences trafficking and is important for correct targeting towards the plasma membrane [23,31,32]. This is presumably due to the fact that all G-family ABC transporters lack a signal peptide but have a short carboxy-terminal tail after the last transmembrane domain which acts as targeting signal for membrane insertion as is the case for type-II transmembrane spanning proteins. Blocking this signal may result in inefficient incorporation of the transporter into and targeting towards the target membranes.

Our results show that ABCG1(666) acts as homodimer. Homodimerization of ABCG1 was earlier concluded also by others, either by indirect means like interference of an ER-retained misfolded ABCG1-mutant with cholesterol export [11], or simply by the fact that overexpression of ABCG1 enhanced cholesterol export, although that observation did not rule out that ABCG1 had been complexed with another half transporter that was present in larger quantities than endogenous ABCG1 [9–12,33]. Recently, homodimerization was shown by coimmunoprecipitation and Western blot detection of coexpressed variants harboring two different epitope tags [12].

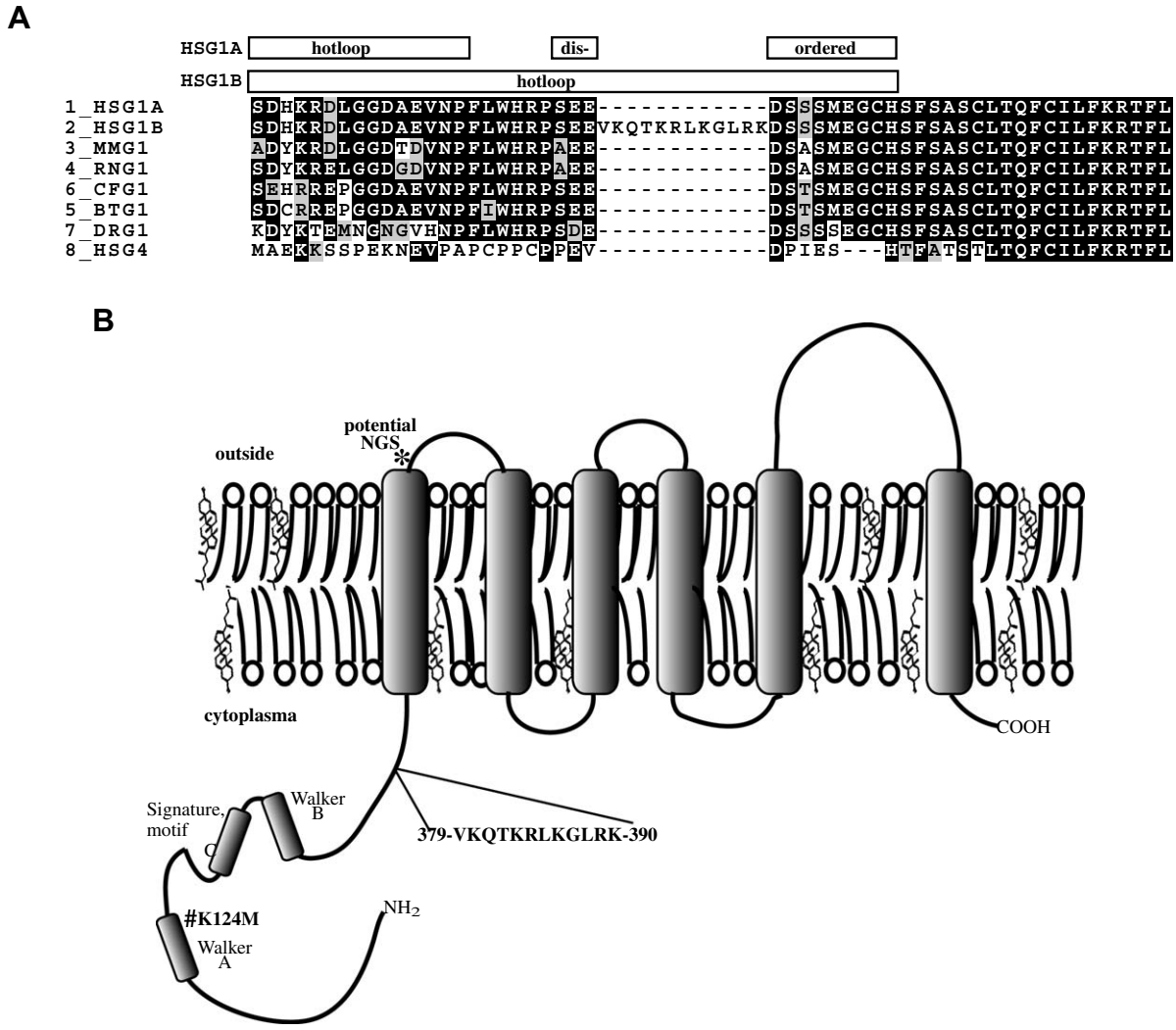

Fig. 8. Insertion of dodecapeptide into ABCG1(666) within a flexible linker region. (A) This multiple sequence alignment shows differences between homologous and orthologous peptide sequences similar to human ABCG1 at the position flanking the alternative splice site at the end of exon 17 [15,16]. Identical amino acids are indicated with black, homologous amino acids with gray boxes. Within this stretch of sequence a region of intrinsic protein disorder is present, as indicated with boxes labeled as "hotloop" or "disordered" according to DisEMBL program within the Simple Modular Architecture Research Tool (SMART) at the EMBL homepage (http://www.smart.embl-heidelberg.de) [34,35]. Following nucleotide database accessions were used for the alignment: HSG1A: *H. sapiens* ABCG1(666) NM_016818.2; HSG1B: *H. sapiens* ABCG1(678) NM_004915.3; MMG1: *M. musculus* ABCG1 NM_009593.1; RNG1: *R. norvegicus* ABCG1 NM_053502.1; BTG1: *B. taurus* ABCG1 XM_587930.2; CFG1: *C. familiaris* ABCG1 XM_544902.2; DRG1: *D. Rerio* ABCG1 XM_679931.1; HSG4: *H. sapiens* ABCG4 NM_022169.3. (B) Shows a schematic topology model of ABCG1. The predicted, potential N-linked glycosylation site (NGS) in human ABCG1 protein is indicated (*). The mutated site in the Walker-A motif of the transporter, used for generating ABCG1(666; K124M) mutant, is indicated as well (#). The 12 amino acid segment present in ABCG1(678) is indicated.

However, that study did not exclude, that ABCG1 formed complexes with other members of the G-family of ABC-transporters, like was shown for the heteromeric ABCG5/ABCG8 complex [17,23]. Another study led to the assumption that ABCG4 and ABCG1 may be able to form a heterodimer, since human ABCG1 ATPase activity in insect cells could be inhibited by expression of human ATPase-deficient ABCG4 [33]. Our results confirm this observation in a more direct manner and exclude that ABCG1 forms complexes with any other ABC-transporter of the G-family.

Our results show that ABCG1(666)-mediated cholesterol export is rather promiscuous with respect to the cholesterol acceptor, since we observed a doubling of cholesterol export to HDL_2, HDL_3 and LDL. However, as has been shown by others for ABCG1(678) [10–12], ABCG1(666) mediated almost no cholesterol efflux if apoAI was used as the acceptor. This differentiates all studied forms of ABCG1 from ABCA1 which has clear acceptor specificity for lipid-free apolipoproteins and not for HDL.

In summary, our data support that ABCG1(666) is a functional ABCG1 variant which may in fact be the most prominent form of functional ABCG1 expressed in the human.

Acknowledgements: We thank Hildegard Huenting for excellent technical assistance with tissue culture work as well as Karin Tegelkamp and Walburga Hanekamp for cloning. We thank Dr. Helen Hobbs (UTSW, Dallas, TX, USA) for providing us with an ABCG5-$(FLAG)_3$ plasmid used as a template for cloning ABCG5 employed in control

experiments. This work forms part of the thesis work of A.L. This work was supported by the Interdisciplinary Center for Clinical Research (IZKF) of the University of Muenster Medical School.

References

[1] Glomset, J.A. (1980) High-density lipoproteins in human health and disease. Adv. Intern. Med. 25, 91–116.
[2] Ross, R. (1999) Atherosclerosis – an inflammatory disease. N. Engl. J. Med. 340, 115–126.
[3] Assmann, G. and Gotto Jr, A.M. (2004) HDL cholesterol and protective factors in atherosclerosis. Circulation 109, III8–III14.
[4] Borst, P. and Elferink, R.O. (2002) Mammalian ABC transporters in health and disease. Annu. Rev. Biochem. 71, 537–592.
[5] Marcil, M. et al. (1999) Mutations in the ABC1 gene in familial HDL deficiency with defective cholesterol efflux. Lancet 354, 1341–1346.
[6] Rust, S. et al. (1999) Tangier disease is caused by mutations in the gene encoding ATP-binding cassette transporter 1. Nat. Genet. 22, 352–355.
[7] Bodzioch, M. et al. (1999) The gene encoding ATP-binding cassette transporter 1 is mutated in Tangier disease. Nat. Genet. 22, 347–351.
[8] Berge, K.E. et al. (2000) Accumulation of dietary cholesterol in sitosterolemia caused by mutations in adjacent ABC transporters. Science 290, 1771–1775.
[9] Nakamura, K., Kennedy, M.A., Baldan, A., Bojanic, D.D., Lyons, K. and Edwards, P.A. (2004) Expression and regulation of multiple murine ATP-binding cassette transporter G1 mRNAs/isoforms that stimulate cellular cholesterol efflux to high density lipoprotein. J. Biol. Chem. 279, 45980–45989.
[10] Wang, N., Lan, D., Chen, W., Matsuura, F. and Tall, A.R. (2004) ATP-binding cassette transporters G1 and G4 mediate cellular cholesterol efflux to high-density lipoproteins. Proc. Natl. Acad. Sci. USA 101, 9774–9779.
[11] Vaughan, A.M. and Oram, J.F. (2005) ABCG1 redistributes cell cholesterol to domains removable by high density lipoprotein but not by lipid-depleted apolipoproteins. J. Biol. Chem. 280, 30150–30157.
[12] Gelissen, I.C. et al. (2006) ABCA1 and ABCG1 synergize to mediate cholesterol export to ApoA–I, Arterioscler. Thromb. Vasc. Biol. 26, 534.
[13] Kennedy, M.A. et al. (2005) ABCG1 has a critical role in mediating cholesterol efflux to HDL and preventing cellular lipid accumulation. Cell Metab. 1, 121–131.
[14] Croop, J.M. et al. (1997) Isolation and characterization of a mammalian homolog of the Drosophila white gene. Gene 185, 77–85.
[15] Chen, H., Rossier, C., Lalioti, M.D., Lynn, A., Chakravarti, A., Perrin, G. and Antonarakis, S.E. (1996) Cloning of the cDNA for a human homologue of the Drosophila white gene and mapping to chromosome 21q22.3. Am. J. Hum. Genet. 59, 66–75.
[16] Kennedy, M.A., Venkateswaran, A., Tarr, P.T., Xenarios, I., Kudoh, J., Shimizu, N. and Edwards, P.A. (2001) Characterization of the human ABCG1 gene: liver X receptor activates an internal promoter that produces a novel transcript encoding an alternative form of the protein. J. Biol. Chem. 276, 39438–39447.
[17] Graf, G.A., Yu, L., Li, W.P., Gerard, R., Tuma, P.L., Cohen, J.C. and Hobbs, H.H. (2003) ABCG5 and ABCG8 are obligate heterodimers for protein trafficking and biliary cholesterol excretion. J. Biol. Chem. 278, 48275–48282.
[18] Havel, R., Eder, H. and Bragdon, J. (1955) J. Clin. Invest. 34, 1345–1353.
[19] Mezdour, H., Clavey, V., Kora, I., Koffigan, M., Barkia, A. and Fruchart, J.C. (1987) Anion-exchange fast protein liquid chromatographic characterization and purification of apolipoproteins A-I, A-II, C-I, C-II, C-III0, C-III1, C-III2 and E from human plasma. J. Chromatogr. 414, 35–45.
[20] Laemmli, U.K. (1970) Cleavage of structural proteins during the assembly of the head of bacteriophage T4. Nature 227, 680–685.
[21] Engel, T. et al. (2004) ADP-ribosylation factor (ARF)-like 7 (ARL7) is induced by cholesterol loading and participates in apolipoprotein AI-dependent cholesterol export. FEBS Lett. 566, 241–246.
[22] Litman, T. et al. (2002) Use of peptide antibodies to probe for the mitoxantrone resistance-associated protein MXR/BCRP/ABCP/ABCG2. Biochim. Biophys. Acta 1565, 6–16.
[23] Graf, G.A., Li, W.P., Gerard, R.D., Gelissen, I., White, A., Cohen, J.C. and Hobbs, H.H. (2002) Coexpression of ATP-binding cassette proteins ABCG5 and ABCG8 permits their transport to the apical surface. J. Clin. Invest. 110, 659–669.
[24] Litman, T., Druley, T.E., Stein, W.D. and Bates, S.E. (2001) From MDR to MXR: new understanding of multidrug resistance systems, their properties and clinical significance. Cell Mol. Life Sci. 58, 931–959.
[25] Xu, J., Liu, Y., Yang, Y., Bates, S. and Zhang, J.T. (2004) Characterization of oligomeric human half-ABC transporter ATP-binding cassette G2. J. Biol. Chem. 279, 19781–19789.
[26] Engel, T., Lorkowski, S., Lueken, A., Rust, S., Schluter, B., Berger, G., Cullen, P. and Assmann, G. (2001) The human ABCG4 gene is regulated by oxysterols and retinoids in monocyte-derived macrophages. Biochem. Biophys. Res. Commun. 288, 483–488.
[27] Devine, S.E., Hussain, A., Davide, J.P. and Melera, P.W. (1991) Full length and alternatively spliced pgp1 transcripts in multidrug-resistant Chinese hamster lung cells. J. Biol. Chem. 266, 4545–4555.
[28] Grailles, M., Brey, P.T. and Roth, C.W. (2003) The *Drosophila melanogaster* multidrug-resistance protein 1 (MRP1) homolog has a novel gene structure containing two variable internal exons. Gene 307, 41–50.
[29] Pauli-Magnus, C. et al. (2004) Sequence analysis of bile salt export pump (ABCB11) and multidrug resistance p-glycoprotein 3 (ABCB4, MDR3) in patients with intrahepatic cholestasis of pregnancy. Pharmacogenetics 14, 91–102.
[30] Chutkow, W.A., Makielski, J.C., Nelson, D.J., Burant, C.F. and Fan, Z. (1999) Alternative splicing of sur2 Exon 17 regulates nucleotide sensitivity of the ATP-sensitive potassium channel. J. Biol. Chem. 274, 13656–13665.
[31] Rocchi, E., Khodjakov, A., Volk, E.L., Yang, C.H., Litman, T., Bates, S.E. and Schneider, E. (2000) The product of the ABC half-transporter gene ABCG2 (BCRP/MXR/ABCP) is expressed in the plasma membrane. Biochem. Biophys. Res. Commun. 271, 42–46.
[32] Scheffer, G.L. et al. (2000) Breast cancer resistance protein is localized at the plasma membrane in mitoxantrone- and topotecan-resistant cell lines. Cancer Res. 60, 2589–2593.
[33] Cserepes, J. et al. (2004) Functional expression and characterization of the human ABCG1 and ABCG4 proteins: indications for heterodimerization. Biochem. Biophys. Res. Commun. 320, 860–867.
[34] Schultz, J., Milpetz, F., Bork, P. and Ponting, C.P. (1998) SMART, a simple modular architecture research tool: identification of signaling domains. Proc. Natl. Acad. Sci. USA 95, 5857–5864.
[35] Linding, R., Jensen, L.J., Diella, F., Bork, P., Gibson, T.J. and Russell, R.B. (2003) Protein disorder prediction: implications for structural proteomics. Structure 11, 1453–1459.